RSC Advances

PAPER

Cite this: *RSC Adv.*, 2016, **6**, 96870

# Metal removal and reduction potential of an exopolysaccharide produced by Arctic psychrotrophic bacterium *Pseudomonas* sp. PAMC 28620†

Ganesan Sathiyanarayanan,[a] Shashi Kant Bhatia,[a] Hyun Joong Kim,[a] Jung-Ho Kim,[a] Jong-Min Jeon,[a] Yun-Gon Kim,[b] Sung-Hee Park,[c] Sang Hyun Lee,[a] Yoo Kyung Lee[d] and Yung-Hun Yang*[ae]

Received 7th July 2016
Accepted 29th September 2016

DOI: 10.1039/c6ra17450g

www.rsc.org/advances

An exopolysaccharide (EPS) was produced from psychrotrophic Arctic glacier fore-field soil bacterium *Pseudomonas* sp. PAMC 28620 using glycerol enriched medium and the maximum productivity 7.24 ± 0.31 g $L^{-1}$ of EPS was obtained after 168 h of fermentation. The EPS was purified and analysed by HPLC, GC-MS, FT-IR, $^{1}H$ and $^{13}C$ NMR. The EPS obtained from Arctic strain PAMC 28620 exhibits a distinctive structural composition and the constituent sugar monomers are rhamnose, galactose, glucose, fucose, mannose and ribose. The purified EPS has shown excellent flocculating and emulsification capacities with promising biotechnological and ecological implications. From the metal removal experiments, the EPS exhibited remarkable metal adsorption (99%) potential adopting the order $Fe^{2+}$ > $Cu^{2+}$ > $Mg^{2+}$ > $Zn^{2+}$ > $Mn^{2+}$ > $Ca^{2+}$. FE-SEM combined with EDX analysis has shown that the metal ions were complexed or immobilized onto the EPS matrix and further reduced to nanoparticles (150–950 nm). This study is significant in terms of metal removal and reduction potential of Arctic bacterial EPS and the possible ecological roles of the EPS in Arctic environment.

## 1. Introduction

Extremophilic bacteria are life forms that thrive in extreme conditions of temperature, pH, ionic concentration (salt/sugar), pressure and ionizing radiation. In particular, most of the bacteria that exist in polar environments produce exopolysaccharides (EPSs) as cryoprotectants to survive in extreme cold weather condition and these bacteria have developed delicate mechanisms that allow them to deal with various kinds of environmental stresses.[1,2] The structural features of some bacterial EPSs from the Arctic and Antarctic environments have been previously studied,[3–7] however, there have been very few reports on their ecological and biotechnological implications.[1,8] Bacterial and algal EPSs are believed to be essential for the aggregate development, adhesion to surfaces, biofilm formation, and nutrient uptake (organic or inorganic) in the Arctic/Antarctic environment.[3,8,9] At present, bacteria from polar regions are being recognized as a rich source of various biological macromolecules that are of special interest towards various biotechnological applications.[7,10] However, there are very few reports on the EPSs from Arctic glacier fore-field soil bacteria and the structure, ecological and biotechnological implications of these EPSs are yet to be identified.

The field of bacterial EPSs is well-established for years and EPSs are well known for numerous viable applications in various industries like pharmaceuticals, food, cosmetics, oil recovery, paper industry, and also in bioremediation.[11,12] Also, there has been a growing interest for the exploration of unique EPSs and some of them are now being sold in market such as bacterial alginates, gellan, pullulan, xanthan, welan, dextran levan *etc.*[11,12] EPS-based polymers are completely biodegradable and their catabolic intermediates are environmentally benign in nature. It has also been reported that most of the bacterial EPSs could act as flocculating, emulsifying, and metal removal (biosorbents) agents in wastewater treatment, hydrocarbon degradation, and heavy metal bioremediation, respectively.[7,13,14] The process of metal bioremediation must be simple, reasonably inexpensive, and ecofriendly in nature.[15] Due to the economic

[a]*Department of Biological Engineering, College of Engineering, Konkuk University, Seoul 143-701, South Korea. E-mail: seokor@konkuk.ac.kr; Fax: +82-2-3437-8360; Tel: +82-2-450-3936*

[b]*Department of Chemical Engineering, Soongsil University, 511 Sangdo-dong, Seoul 156-743, South Korea*

[c]*Food Ingredients Center, Foods R&D, CheilJedang, Guro-dong, Guro-Gu, Seoul 152-051, South Korea*

[d]*Division of Life Sciences, Korea Polar Research Institute, 26 Songdomirae-ro, Yeonsu-gu, Incheon, 21990 South Korea*

[e]*Institute for Ubiquitous Information Technology and Applications Konkuk University, Seoul 143-701, South Korea*

† Electronic supplementary information (ESI) available. See DOI: 10.1039/c6ra17450g

concern, EPSs can be utilized as effective biosorbents for removing heavy metals from the polluted environments. Therefore, EPSs with flocculating, emulsifying, and metal-binding capabilities are of specific concern for several biotechnological industries.

Recent literatures evidenced that the bacterial EPSs are excellent metal-binding agents to attract trace and toxic metal ions such as Cu, Cr, Pb, Co, Zn, Ni, Cd, Al and Fe.[16–20] Most of the EPS–metal binding studies were focused on the commercial viewpoint, and only few have systematically addressed the ecological implications of EPS–metal complexes in natural ecosystems.[1,21,22] EPS-based metal binding/removal is a unique metabolism-independent bio-adsorption process due to the formation of interfaces between metal cations and the poly-anionic chelating functional groups (*i.e.*, hydroxyl, carboxyl and amino groups) of the EPS.[20,23] Furthermore, a physico-chemical communication between the metal cations and EPS functional groups may also be established by physical sorption, immobilization, ion exchange complexation, and precipitation processes.[20,24] In recent years, the polyanionic nature of bacterial EPS has been a subject of interest and their role in biogeochemical processes especially metal cycling in extreme natural environment is still unclear. So far, there is no report on the direct and critical analysis of EPS–metal binding properties under surface-interface level except quantification.

In our previous work, we have shown that cryoprotective nature of EPS purified from *Flavobacterium* sp. ASB 3-3 isolated from Arctic glacier fore-field soil. We have also found that some other Arctic strains including AS-06/29 is able to produce EPS effectively.[3] In this study, Arctic glacier soil bacterium *Pseudomonas* sp. PAMC 28620 (strain AS-06/29) was used as model strain to produce EPS since fluorescent pseudomonads are commonly linked with metal resistance[25–27] and also known for the production of large amounts of functionally diverse EPSs.[28–31] These special features have raised questions regarding their role in metal-binding and metal reduction. Therefore, in this study, the detailed structural components of the EPS produced by the strain PAMC 28620 were elucidated and its emulsifying and flocculating properties were also evaluated with the intention of exploring the possible ecological roles of the EPS in Arctic environment. In addition, metal removal, complexation and reduction capacities of the purified EPS were analyzed and its ecological and biotechnological implications have also been discussed.

## 2. Experimental methods

### 2.1. Microorganism, screening and identification of EPS producing Arctic strain PAMC 28620

All experiments were performed in compliance with the relevant laws and institutional guidelines of Konkuk University, Seoul, South Korea and also under guidelines of Institutional Biosafety Committee (IBS) at Konkuk University (LML09-165). In addition, this study and protocols were approved by the Institutional Review Board of Ethics Committee of Konkuk University. All procedures were carried out according to rules and regulations provided by the Institutional Review Board/Ethics Committee of Konkuk University, Seoul, South Korea. The bacterial strain AS-06/29 was isolated from Arctic glacier soil collected from Midtre Lovenbreen, Ny-Ålesund in Svalbard and the field campaign was permitted by Svalbard Science Forum (RIS ID: 6752). The Arctic bacterial strain AS-06/29 has been deposited into Korea Polar Research Institute (KPRI) based Polar and Alpine Microbial Collection (PAMC) center under the general deposit category with the accession number PAMC 28620. Strain PAMC 28620 was cultivated on nutrient and LB medium (Miller) at 25 °C for one week and then cryopreserved at −74 °C. EPS synthesis was initially evaluated by using a modified nitrogen-limited broth[32] containing 20 g glucose, 1.5 g $NH_4NO_3$, 0.3 g yeast extract, 2.0 g $K_2HPO_4$, 0.3 g $KH_2PO_4$, 0.2 g $MgSO_4 \cdot 7H_2O$ and 0.1 g NaCl in 1 L water. Strain PAMC 28620 was cultured in an Erlenmeyer flask (250 mL) comprising 50 mL of nitrogen-limited medium and then incubated for 96 h at 25 °C with agitation of 200 rpm. The cell free supernatant (CFS) was pooled; EPS was separated by ethanol precipitation and estimated by phenol-sulfuric acid assay.[33] The bacterial strain PAMC 28620 was identified based on the morphological and biochemical features and then compared with Bergey's manual of systematic bacteriology.[34] Agarose and bacterial agar were supplied from the Microbial carbohydrate resource bank at Konkuk University, South Korea. For phylogenetic identification, the genomic DNA was extracted and around 1.5 kb of 16S rRNA gene was amplified with universal degenerate primers 27F (5′-aga gtt tga tcc tgg ctc ag-3′) and 1492R (5′-ggt tac ctt gtt acg act t-3′).[35] The PCR amplicon was cloned by using TOPO TA cloning kit according to manufacturer guidelines (Invitrogen) and then sequenced. 16S rRNA gene (sequences) obtained from the strain PAMC 28620 was compared with other eubacterial 16S rRNA gene sequences by using NCBI BLAST (http://www.blast.ncbi.nlm.nih.gov/Blast.cgi) for their pair-wise identities. Multiple sequence alignment was carried out by using ClustalW2 version of EBI (http://www.ebi.ac.uk/Tools/msa/clustalw2/) with 0.5 transition weight. Phylogenetic trees were constructed with MEGA version 6.06 (http://www.megasoftware.net) using neighbor joining (NJ) algorithm. Moreover, ribosomal database project (RDP-11) (http://www.rdp.cme.msu.edu/) also used to find out the taxonomic identity of the strain by *seqmatch* and *classifier* program. The partial sequences of the 16S rRNA gene of strain PAMC 28620 has been deposited into GenBank under accession number KT445272.

### 2.2. Production, extraction and purification of EPS from Arctic strain PAMC 28620

A single colony of strain PAMC 28620 was cultured in 50 mL of LB medium (Miller) to prepare the pre-inoculum for the mass production. The EPS mass production was conducted in 2 L Erlenmeyer shaker flask comprising 800 mL of production medium-2 (PM-2) and 80 mL of pre-inoculum. The PM-2 is a modified version[3] which includes glycerol 30 g $L^{-1}$, yeast extract 2.0 g $L^{-1}$, $NH_4H_2PO_4$ 3.0 g $L^{-1}$, $K_2HPO_4$ 4.0 g $L^{-1}$, $KH_2PO_4$ 1.5 g $L^{-1}$, $MgSO_4 \cdot 7H_2O$ 0.015 g $L^{-1}$, and trace element solution (TES) 1 mL $L^{-1}$ with initial pH 7.0 ± 0.2. The culture flasks with production medium were incubated at 25 °C for 192

h with 150 rpm agitation. Around 10 mL of cultured broth was periodically collected and used to monitor the growth of bacteria in terms of optical density (OD) at 590 nm, biomass, EPS yield, pH change, flocculating and emulsifying activity of the CFS during the fermentation process. Flocculation and emulsification activities were examined according to the methods described in previous studies.[3,36] All the experiments were performed in triplicate and the results were represented as mean ± standard deviation (SD) ($n = 3$).

After 192 h of incubation, the spent culture was centrifuged at 8000×*g* for 20 min and resulting biomass was weighed (dry cell weight). The CFS was heated at 80 °C for 1 h to deactivate the EPS degrading enzymes. The pooled CFS was concentrated into 1/10 volume using a rotary evaporator (Eyela World, Tokyo Rikikai Co., Ltd). For the extraction and purification of EPS, about three volume of pre-chilled alcohol (96% ethanol) was mixed with CFS and incubated at −20 °C for 4 to 5 hours and then centrifuged at 10 000×*g* for 20 min to collect EPS precipitate. The EPS precipitate was deproteinized[3,8] and dialyzed against HPLC grade water. The EPS was further purified by Dowex column chromatography with 200–400 mesh (Sigma-Aldrich) and styrene-divinyl benzene as matrix gel and the purified fraction was concentrated, lyophilized and stored at 4 °C.

### 2.3. Chemical characterization of EPS

The chemical constituents of the EPS were identified by using series of chemical assays along with chromatographic and spectroscopic methods. About 100 mg of unpurified crude EPS was dissolved in HPLC grade water and the total carbohydrate and protein contents were determined by phenol-sulphuric acid method[33] and Bradford assay[37] using glucose and bovine serum albumin (BSA) as standard, respectively. The sulfate content was estimated using $K_2SO_4$ as standard according to the method described in previous literature.[38] The purified EPS solution was scanned (200–800 nm) under UV and visible (UV/Vis) spectrophotometer (Amersham Biosciences, Inc.). Purity analysis was performed on high performance liquid chromatography (HPLC) (Agilent) with an Aminex HPX-87H column (Bio-Rad, Hercules, CA), coupled to an ultraviolet (UV at 210 nm) and refractive index (RI) detector, using 5 mM sulfuric acid ($H_2SO_4$) as eluent, at a flow rate of 0.600 mL $min^{-1}$.

Glycosyl composition was identified by using gas chromatography-mass spectrometry (GC-MS).[8] The purified EPS sample (20 mg) was hydrolyzed with 1 mL of 99% trifluoroacetic acid (TFA) at 125 °C for 2 h. The hydrolyzate was dried and washed twice with 500 μL of methanol. Derivatization was performed by adding 30 μL methyloxyamine in pyridine (20 mg $mL^{-1}$) and incubated at 70 °C for 10 min, followed by addition of 70 μL of *N*-methyl-*N*-(trimethylsilyl) trifluroacetamide (MSTFA) and incubated at 70 °C for 10 min. The derivatized sample was then dissolved in chloroform and 1 μL of sample was automatically injected into the Clarus 680 GC-MS (PerkinElmer, USA) equipped with triple axis detector carrying Elite 5 ms column (30 mm length, 0.25 mm internal diameter, 0.25 mm film) at a split ratio of 10 : 1 with column flow 1.0 mL $min^{-1}$. The injector temperature was set at 280 °C while the oven and column temperatures were programmed as 60 °C for 2 min, then increased to 140 °C at the rate of 2 °C $min^{-1}$, held for a second, and again increased to 300 °C at 20 °C $min^{-1}$ to hold at the temperature for 10 min. Standard monosaccharides (Sigma-Aldrich) were used as the reference for peak retention time and ionization mass determination.

To identify the major functional groups that are present in the purified EPS, Fourier transform infrared (FT-IR) spectroscopy (Tensor 27, Bruker Corporation) was employed. Double sided FT-IR transmittance was measured in spectral range of 600–4000 $cm^{-1}$ with a data resolution of 4 $cm^{-1}$. Nuclear magnetic resonance (NMR) spectra were obtained using a Bruker Avance II 500 MHz spectrometer (Bruker Co., Billerica, MA) with a 5 mm pulsed field gradient (diffusion) probe. The EPS sample was deuterium exchanged by dissolving the sample in $D_2O$ at concentrations of 5 mg $mL^{-1}$ and 20 mg $mL^{-1}$ for $^1H$ NMR (500 MHz) and $^{13}C$ NMR (150 MHz), respectively.

### 2.4. Emulsification activity of the EPS

Emulsification activity of purified EPS (1%) was analyzed by adding toluene (99%, Samchun) into EPS solution (5%) in a ratio of 1 : 1 and then vortexed for 2 min. The vortexed solution was allowed to stand for 24 h at room temperature. After 24 h incubation, the height of the emulsified layer was measured and the emulsification index ($EI_{24}$ in %) was calculated using a formula: $EI_{24} = (H_{EL}/H_S) \times 100$. Where, $H_{EL}$ is height of the blended (emulsified) layer and $H_S$ is the height of the total fluid content.[39] The same method was also used to measure the $EI_{24}$ of the EPS against with hydrocarbons including *n*-hexane (95%, Samchun), *n*-hexadecane (99%, Alfa Aesar), petroleum (~18%, Sigma-Aldrich), methyl octonate (99%, Aldrich), and methyl 10-undecanoate (96%, Sigma-Aldrich). Chemical surfactants like sodium dodecyl sulfate (SDS) (anionic) and Triton X 100 (nonionic) were used as positive controls (1%) to compare with EPS.

### 2.5. Flocculation properties of the EPS

The flocculating activity was determined by using a solution of natural kaolinite (kaolin clay) ($Al_2Si_2O_5(OH)_4$; Sigma-Aldrich). In brief, 4 mL of $CaCl_2$ (1% w/v) and 200 μL of EPS polymer (5 g $L^{-1}$) were mixed with 50 mL (5 g $L^{-1}$) of kaolin clay solution (pH 8.0) and then slightly agitated for 2 min and left to stand for 5 min at room temperature (25 °C). Clear aqueous phase was separated and its OD was measured (550 nm) by using a 96-well plate reading UV/visible spectrophotometer (Sunrise™-Tecan). The flocculating efficacy (fe) in percentage (%) was calculated by using the formula: $f_e = b - a/b \times 100$, here '*b*' and '*a*' are $OD_{550\ nm}$ of the EPS sample and control (distilled water instead of EPS), respectively.[40] The impact of the polymer dosage (10–100 mg $L^{-1}$), pH (3–12), temperature (5–50 °C), and metal cations (0.09 M of NaCl, $ZnCl_2$, $MnCl_2$, $MgCl_2$, KCl, $FeCl_3$, and $CuCl_2$) on the flocculation mechanism were also evaluated. All these experiments were conducted in triplicate keeping the following parameters as constants: EPS 50 mg $L^{-1}$, pH 7.0, temperature 25 °C, and $Ca^{2+}$ cation.

### 2.6. Metal tolerance property of Arctic strain PAMC 28620

Metal tolerance was evaluated based on the minimum inhibitory concentration (MIC) of metals against to strain PAMC 28620. The MIC was determined in LB broth (Miller) amended with 0.1, 0.5, 1.0, 1.5 to 5.0 m mol $L^{-1}$ of $Fe^{2+}$, $Cu^{2+}$, $Zn^{2+}$, $Ca^{2+}$, $Mn^{2+}$ and $Mg^{2+}$ as an individual experiments. Metal supplemented bacterial cultures were incubated for 2 weeks at 25 °C under shaking (200 rpm) and further bacterial growth was checked (OD at 590 nm) for every 24 h. MIC was estimated by means of the first dilution which entirely prevents bacterial growth in LB broth.[41]

### 2.7. Metal-binding properties of the EPS

Batch biosorption experiment (one-metal system) was conducted to study about the metal-removal potential of the purified EPS. Selected metal cations such as $Fe^{2+}$, $Cu^{2+}$, $Zn^{2+}$, $Ca^{2+}$, $Mn^{2+}$ and $Mg^{2+}$ (corresponding metal salts) were prepared (50 mg $L^{-1}$) with HPLC grade deionized water and 4 mL of EPS (50 mg $mL^{-1}$) was mixed with 4 mL of the selected metal ion solutions and each solution was finally made up to 12 500 mg $L^{-1}$ of concentration. The EPS–metal solution was kept at 25 °C for 72 h under agitation (150 rpm). After incubation, one volume of ethanol was added to the EPS–metal solution to collect the EPS and then centrifuged at 8000×*g* for 20 $min^{-1}$. The unbound metal ions were removed from the EPS by overnight dialysis against deionized water. The ethanol precipitated EPS was dried and stored at room temperature until FE-SEM-EDX analysis. About 3 mL of EPS-free aqueous solution was filtered and injected into inductively-coupled plasma atomic/optical emission spectrometry (ICP-AES/OES) (Perkin Elmer Life and Analytical Sciences, Inc., MA, USA) to determine the residual metal concentration. The unbound metal ions were also considered for the final residual metal ion calculation. The metal removal capacity of the EPS was calculated by using the formula: $Q = \text{Vol}\ (C_i - C_f)/m$, where $C_i$ is initial metal ion concentration in aqueous solution of volume Vol, where $C_f$ is the equilibrium level of metal in aqueous solution and $m$ is the quantity (mass) of EPS.[17] The metal-binding experiments were performed without any interference of pyoverdin (PVD), since PVD produced by fluorescent pseudomonads has the ability to adsorb range of metal ions including iron (Fe). Therefore, PVD was assessed only for identification purposes and it was removed from the CFS while extracting the EPS.

### 2.8. FE-SEM and EDX spectroscopy analysis

The metal ion and EPS interaction was critically analyzed by field-emission scanning electron microscope (FE-SEM) linked with energy dispersive X-ray spectroscopy (EDX or EDS) (JSM-6700F, JEOL Ltd., Japan). The samples such as pure and metal enriched EPS were immobilized on a microscopic aluminum stump using a carbon coated glue tape. Additionally, the EPS samples were hard-pressed to get an even and flat exterior based on the necessities of the international standards of EDX analysis. After fabrication, the samples were coated with platinum and the typical EDX spectra with SEM images were obtained from five random zones of every sample.[20]

## 3. Results and discussion

### 3.1. Identification of Arctic strain PAMC 28620

The strain PAMC 28620, isolated from glacier soil of Arctic, was characterized using morphological, cultural, biochemical and other physiological attributes (Table S1†). Strain PAMC 28620 is a rod-shaped, Gram-negative and facultative anaerobe. When grown on *Pseudomonas* agar, the colonies seemed to be globular, oily, viscid, and milky in color. The strain also produces a fluorescent pyoverdin (PVD) siderophore when the medium is depleted with essential trace metal ions (Fig. S1†). NCBI-BLASTn examination designated that the 16S rRNA gene sequence (1437 bp) of PAMC 28620 is 99% related to the strain *Pseudomonas* sp. NR 6-02 (GenBank accession no: KM253127.1). The supreme homologous (98–99%) 16S rRNA reference gene sequences were retrieved from GenBank and neighbor-joining phylogenetic tree was constructed (Fig. S2†). The morphological and biochemical characteristics together with the phylogenetic analysis indicate that the Arctic strain PAMC 28620 belongs to genus *Pseudomonas*. The strain PAMC 28620 can grow well at even low temperature and exhibited its optimal growth between the temperature ranges of 15 °C to 25 °C (Fig. S3†). In recent decades, only few EPSs producing psychrophilic and psychrotrophic bacterial strains including *Pseudoalteromonas* (strain SM20310, SM9913, CAM025 & CAM036), *Shewanella* sp. CAM090, *Flavobacterium* (strain CAM005 & ASB 3-3), *Polaribacter* (strain SM1127 & CAM006), and *Colwellia psychrerythraea* 34H were isolated from Arctic and Antarctic environment.[1–4,7,8,42,43]

### 3.2. Growth characteristics and EPS production from Arctic strain PAMC 28620

Arctic strain PAMC 28620 grew well on solid media (LB & NA) and in liquid (LB & PM-2) mediums at 25 °C for 5 to 7 days of incubation. Fig. 1A shows a typical biomass, pH change and EPS production in 3% glycerol supplemented medium (PM-2). Emulsification and flocculating activity along with optical density of the culture are depicted in Fig. 1B. The log phase has started instantly after seeding the pre-inoculum and attaining a maximum bacterial growth ($OD_{590\ nm}$ 3.76 ± 0.15) at 168 h of cultivation (Fig. 1B). This fluctuation in bacterial growth was combined with a proportionate decline of the pH of the culture medium (192 h), as of 7.07 ± 0.01 to 6.36 ± 0.05. EPS synthesis was initiated at the time of early exponential phase (24 h) and amplified utmost quickly during late log phase and gradually afterward. The maximum EPS production (7.24 ± 0.31 g $L^{-1}$) was obtained at late stationary phase (168 h) and it has strong coexistence with maximum biomass yield around 8.74 ± 0.14 g $L^{-1}$. This EPS productivity was similar to that of our earlier study on Arctic *Flavobacterium* sp. ASB 3-3, wherein EPS yield was about 7.25 ± 0.26 g $L^{-1}$ at 120 h of incubation.[3] After 72 h of cultivation, the EPS production was quite oscillatory and it continued until 192 h with minor fluctuations in the EPS productivity. When the medium was seeded with 1% inoculum, the growth curve was suddenly moved to log phase rather than crossing over an apparent lag phase. The maximum yield of EPS

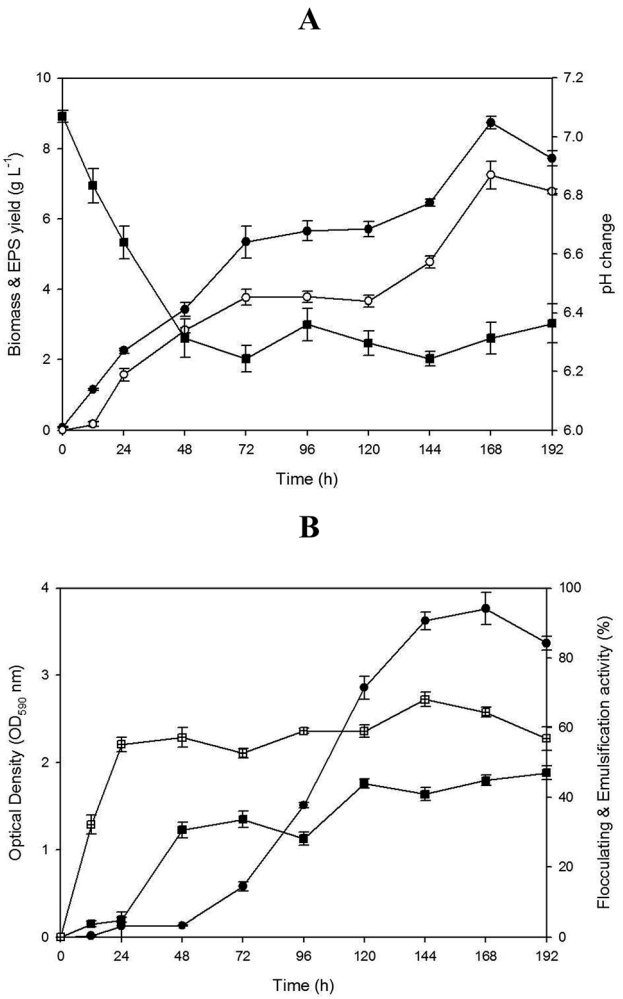


Fig. 1 EPS production from *Pseudomonas* sp. PAMC 28620. (A) Biomass (●), pH change (■) and EPS production (○) in 3% glycerol enriched medium. (B) Emulsification (⊞) and flocculating activity (■) of the cell free supernatant (CFS) along with optical density of bacterial growth (●) had shown to correlate with their emulsification and flocculation activities. The values shown are means ± SDs from three independent experiments.

observed at the end of the stationary phase. Meanwhile, the EPS production and bacterial growth were run-parallel and a typical death phase was not observed in PAMC 28620. The emulsifying activity of the EPS has begun after 12 h, overlapping with the optical density and then reached maximum level ($EI_{24}$ of 64.41 ± 1.09) at the stationary phase (168 h) (Fig. 1B). The CFS has produced fine emulsions with small and uniform in sizes (below 100 μm) and emulsions were stable for several weeks at room temperature. The flocculating activity of the CFS was reached its maximum about 47.05 ± 1.63% during the late stationary phase (192 h) of the bacterial growth.

### 3.3. Chemical and structural analysis of the EPS

The total carbohydrate, protein and sulfate contents were determined as 521.72, 318.86 and 159.42 mg $g^{-1}$, respectively from the unpurified crude EPS. The purified fraction of EPS was subjected to UV/Vis absorption and resulting no absorption peak at 280 nm or 260 nm, thus demonstrating the absence of DNA and protein contamination. It was observed that a single peak during the HPLC analysis and it confirmed that the EPS sample was pure, absolutely free of impurities (Fig. S4†). Glycosyl analysis has revealed the principal components of the EPS are rhamnose, galactose, glucose, fucose, mannose and ribose (Fig. 2A). However, the ecological implication of rare sugars (fucose, mannose & ribose) in the EPS is quite unknown. The detailed compositions of carbohydrate and the molar percentage of each monosaccharide are shown in Table 1. Mass spectrum (MS) of the each monosaccharide is displayed in Fig. S5.† Most of the EPSs produced by Arctic/Antarctic bacteria are mainly composed of α-mannose, *N*-aetylglucosamine (GlcNAc), and uronic acids (10–50%) as the key monomers along with amino sugars, amidated residues, and ketal-linked pyruvate.[4,7,8] Some inorganic constituents like sulfate and phosphate groups may also be present in EPSs.[4] However, the EPS obtained from PAMC 28620 did not possess any such GlcNAc, uronic acids, and other inorganic substances. Hence, the EPS structural differences amongst the bacteria from polar region are needed to be focused to explore their ecological implications which linked with their chemical composition.

The FTIR spectrum has exhibited a different range of adsorption signals from 3500 to 600 $cm^{-1}$. The strong over-extended signal at 3271 $cm^{-1}$ showed the presence of enormous number of hydroxyl (O–H) groups thereby confirming the typical carbohydrate nature of purified polymer (Fig. 2B). Two more solid peaks at 2930 and 2873 $cm^{-1}$ were assigned to asymmetric and symmetric starches of methylene ($CH_2$) and methyl ($CH_3$) groups, respectively. A sharp adsorption peak at 1644 $cm^{-1}$ and a weak signal at 1550 $cm^{-1}$ were revealing the presence of carboxyl (–COOH) and carbonyl (C═O) groups, respectively. A solid balanced symmetrical stretching signal at 1281 $cm^{-1}$ have confirmed the presence high level of carbonyl (C═O) group of the carboxyl (–COOH) moieties. The stretching band at 1044 $cm^{-1}$ is a typical signature of carbohydrate molecules and a strong signal at 855 $cm^{-1}$ ascertains the presence of polysaccharide glycosidic linkages. The overall FT-IR spectrum has confirmed the complex polymeric nature of purified EPS and these functional groups are believed to be involved in metal binding and metal reduction.[20,32,44]

The 600 MHz $^1$H NMR spectrum of the EPS was complex due to the convergence of most sets of the signals in the region 3.37 to 4.15 ppm (Fig. 3A and S6†). $^1$H NMR spectrum showed six major signals at the area of β-anomeric protons as $\delta$ 5.9 (quadruplet), 5.42, 5.3 (doublet), 5.1 (quadruplet), 5.05, and 4.99 ppm. These anomeric proton resonances indicate the presence of six different kinds of monomeric sugars in the purified EPS. Signals from $\delta$ 1.26 to 1.39 ppm, were assigned to $-CH_3$ of the pyranosyl and furanosyl residues. A strong signal at $\delta$ 1.87 ppm indicates the presence of alkyl $-CH_2-$ protons. The tertiary carbon hydrogen (R–C**H**–OR′) was observed as a multiplet at $\delta$ 4.6 to 3.6 ppm. A signal at $\delta$ 3.5 and 3.2 ppm exposes the presence of methoxy ($-OCH_3$) functional group and acid functional group –OH proton, respectively. The resonance at $\delta$ 5.3 and 5.1 ppm were attributed to α-D-galactose and α-D-glucose.

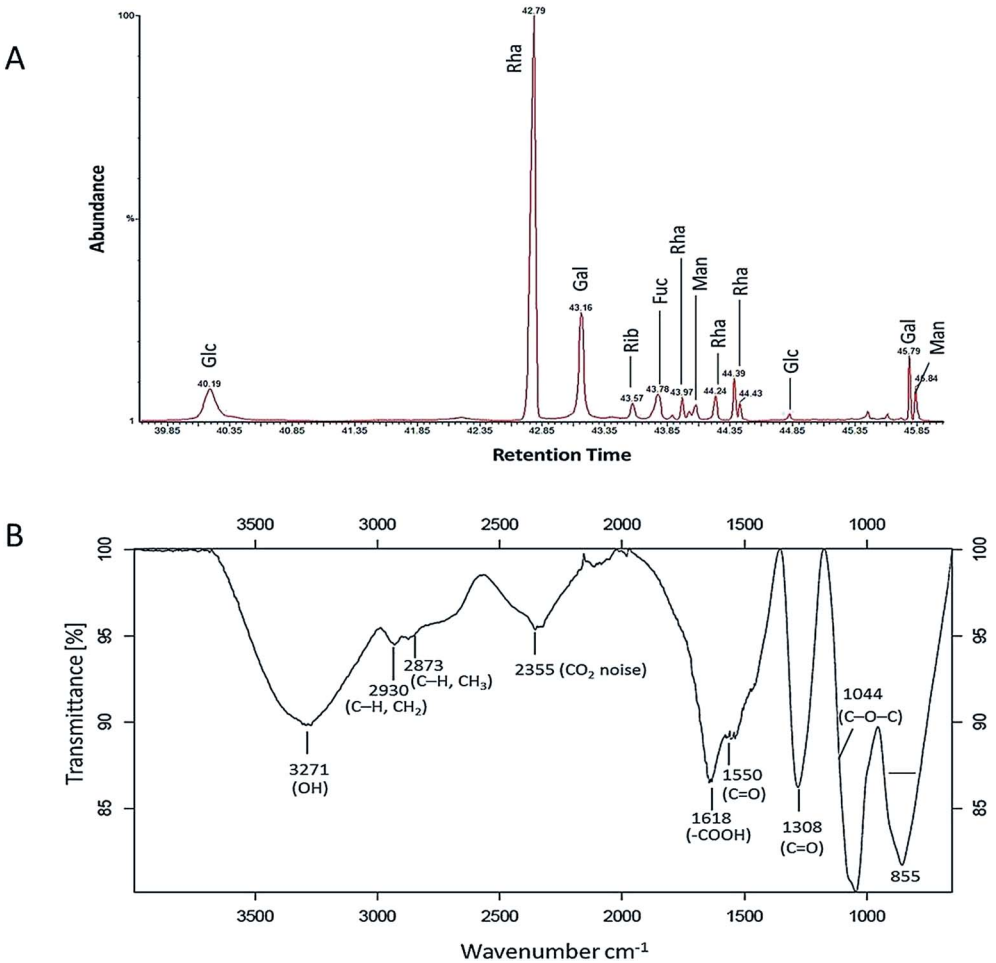


Fig. 2 Characterization of EPS produced by *Pseudomonas* sp. PAMC 28620. (A) GC spectrum of monosaccharide composition analysis of the EPS from strain PAMC 28620. Glc, glucose; Rha, rhamnose; Gal, galactose; Rib, ribose; Fuc, fucose; Man, mannose. (B) FT-IR spectrum of the EPS. The spectrum was recorded around 4000–650 $cm^{-1}$.

Table 1 Glycosyl composition of the EPS from Arctic glacier soil bacterium *Pseudomonas* sp. PAMC 28620

| Glycosyl residue | Amount[a] (mol%) |
|---|---|
| Rhamnose (Rha) | 57.94 |
| Galactose (Gal) | 18.37 |
| Ribose (Rib) | 1.67 |
| Mannose (Man) | 3.78 |
| Glucose (Glc) | 14.30 |
| Fucose (Fuc) | 3.91 |

[a] Approximate mole percent in total purified carbohydrates.

The signal at $\delta$ 4.80 and 4.61 ppm were consigned to α-D-galactose reduced end-chain. The resonances at $\delta$ 4.91 to 4.21 ppm shifts were typical for D-glucose and D-galactose, respectively. The signals at $\delta$ 4.99 to 5.5 ppm were assigned to mannose and ribose residues. In $^1$H NMR, most of the proton signals shares the same region since the monosaccharides (glucose, galactose and mannose) detected in this study are epimers.

The full $^{13}$C NMR spectrum of EPS is shown in Fig. S7† and the peak assigned enlarged spectrum is displayed in Fig. 3B. The resonances appearing above 95 ppm were typical of anomeric carbons [C (1)] involved in (1 → *n*) linked sugar fragments, where *n* = 2, 3, 4 or 6 in our case. C (1) α and β resonances appearing at $\delta$ 103, 75, 99.29, 98.74, 96.82, 96.63, 96.34, 95.13, and 94.93 ppm were identified, and assigned to C (1)-α-fucose, C (1)-α-glucose, C (1)-β-galactose, C (1)-β-glucose, C (1)-α-galactose furanose, C (1)-β-ribose, C (1)-β-mannose and C (1)-β-rhamnose, respectively. C (4) and C (5) of monosaccharides were usually in the region close to $\delta$ 70 to 85 ppm and these chemical shifts are usually interchangeable for all hexoses. The most intense resonance signals around to $\delta$ 70.00 to 74.91 ppm were assigned as C (2) and C (3). C (6) carbon of the each monosaccharide was identified from the signals around $\delta$ 63.43 to 63.58 ppm. A very weak $^{13}$C resonance signal at $\delta$ 19.6 (doublet) was observed and further it was assigned as C (6) $H_3$ side groups of the rhamnose and fucose. Based on the $^{13}$C NMR spectrum, the key structural constituents of EPS were detected as rhamnose, galactose, glucose, fucose, mannose, and ribose. Generally, the chemical shifts around ~60 to 90 ppm were related with secondary alcohols of carbohydrates, whereas 95 to 106 ppm corresponds to the glycosidic carbon of

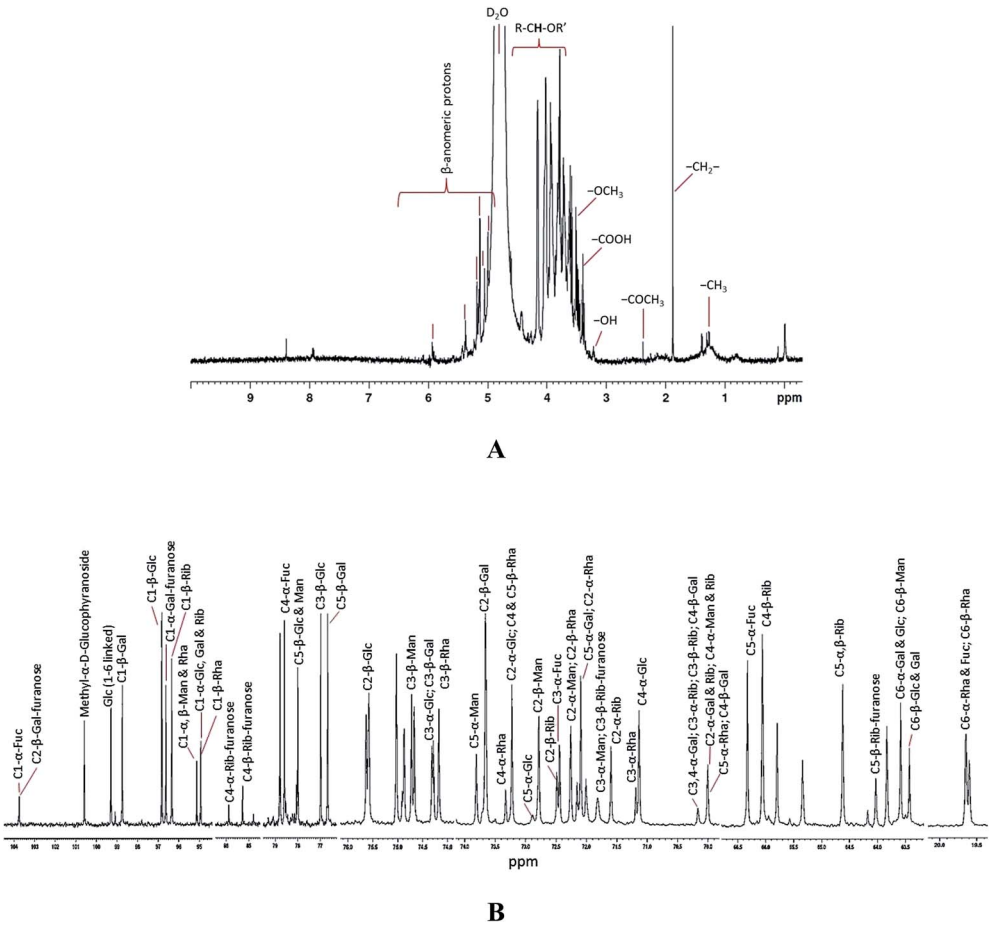


Fig. 3 $^{1}H$ (A) $^{13}C$ (B) NMR spectra of the EPS purified from *Pseudomonas* sp. PAMC 28620. Both NMR spectra were enlarged (magnified) for peak assignment and the full NMR ($^{1}H$ & $^{13}C$) spectra are given as ESI (Fig. S6 and S7†). Glc, glucose; Rha, rhamnose; Gal, galactose; Rib, ribose; Fuc, fucose; Man, mannose; α and β indicates the pyranose.

polysaccharides rings. The glycosidic linkages between the carbon atoms thorough α and β oxygen were detected from the frequencies in the range from ~95 to 103 and ~103 to 106 ppm, respectively. There was neither lipid (~0 to 40) nor peptide (~170) vibrations in $^{13}C$ NMR spectrum and moreover there was no background noise in both $^{1}H$ and $^{13}C$ NMR spectra, thus indicating the purity of the EPS sample. The monosaccharide composition procured from NMR experiments was consistent with the results of glycosyl composition obtained from GC-MS analysis (Table 1). A complete understanding about the structural composition of Arctic bacterial EPSs is significant for revealing their ecological roles and discovering their biotechnological implications. In this study, EPS purified from PAMC 28620 has unique structural composition which different from that of the EPSs secreted by Arctic bacterial strains[3,8,43] and other bacterial extremophiles.[7,45]

### 3.4. Flocculation and emulsification properties of EPS

The required amount of EPS to be used for succeeding flocculation experiments was identified by inspecting various EPS doses in between 10–100 mg $L^{-1}$ as shown in Fig. 4A. While increasing the EPS concentration, the flocculation efficacy was also increased. The maximum flocculating activity about 71.17 ± 2.21% was observed with 70.0 mg $L^{-1}$ of EPS concentration. A slight decrease in flocculation at 100 mg $L^{-1}$ was observed due to EPS saturation resulting in flocs formation and about 300 to 500 μm flocs were molded by the bacterial EPS when tested with kaolinite. The correlation between temperature and flocculation efficacy has remained moderately stable while increasing the temperature (Fig. 4B). The maximum flocculating activity about 72.91 ± 2.54% was observed at 30 °C and the flocculating activity was remaining nearby 62.74 ± 2.43% after the treatment at 50 °C. The flocculation activity was considerably enhanced by both trivalent and divalent cations such as $Fe^{3+}$ (69.95 ± 1.61%), $Mg^{2+}$ (66.05 ± 0.55%), $Mn^{2+}$ (65.66 ± 2.04%), $Ca^{2+}$ (62.77 ± 3.12%), $Cu^{2+}$ (62.41 ± 2.14%) and inhibited to limited extents by $Zn^{2+}$, $Na^{+}$, and $K^{+}$ (Fig. 4C). The highest flocculation was attained at pH 9 with 68.33 ± 3.81% and the efficacy was quite stable in both acidic (pH 3) and basic solutions (pH 12) (Fig. 4D). Emulsification potential of purified EPS along with chemical surfactants (controls) was checked against (pH 7) with six different hydrocarbons (Fig. S8†). The maximum emulsifying activity ($EI_{24}$) was observed against with toluene and methyl octanoate with 67.23 ± 2.07% and 66.69 ± 3.20%, respectively. The obtained $EI_{24}$ values were relatively equivalent

 

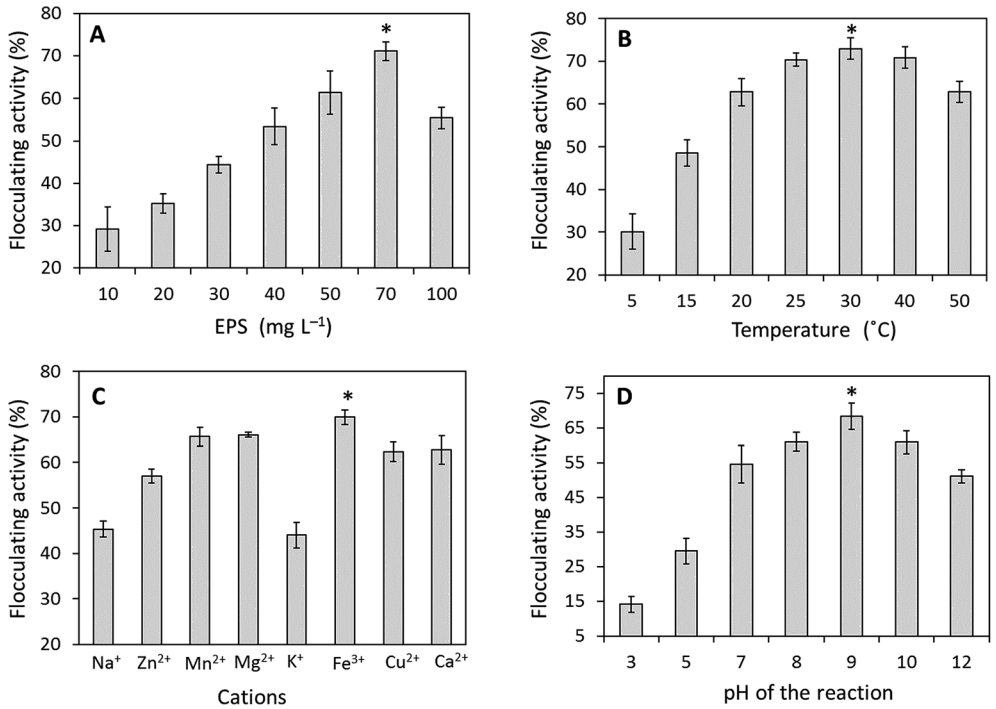


Fig. 4 Flocculation properties of the EPS obtained from Arctic *Pseudomonas* sp. PAMC 28620. Effect of EPS concentration (A), temperature (B), cations (C), and pH (D) on the flocculating activity (%) (mean ± SD) of the EPS. Constant invariables: 50 mg $L^{-1}$ of EPS, pH 7, $Ca^{2+}$ and 25 °C. (*) Flocculating activity is significant at $P < 0.05$.

to the values obtained from the chemical surfactants such as SDS (75.54 ± 2.28 & 56.90 ± 1.17%) and Triton X 100 (66.09 ± 1.64 & 51.69 ± 1.84%), respectively.

It has been believed that some cold-adapted polar bacterial populations are depending primarily on proteins (*i.e.*, amino acids), rather than on carbohydrates, for carbon and energy.[46,47] EPSs secreted by Arctic bacteria may act as colonizing factor to grow on protienaceous particles in the polar environment.[1,47] The flocculation experiment on the EPS produced by strain PAMC 28620 suggested that could be an excellent flocculating agent and also has high ability to adhere to suspended particles in the surrounding medium, indicating that the EPS could adhere to proteinaceous particles in the polar environment when it is secreted by cold-adapted bacteria. Moreover, EPS from strain PAMC 28620 is a polyanionic compound due to its functional groups and this feature may also responsible for the high mucous polysaccharide development thus providing the flocculating and emulsification potential to EPS.[3,48,49] Mostly, flocculation and emulsification properties of the EPSs are ecologically important in terms of development of aggregates and adhesion to ice surfaces, thus also provides protection to bacteria in cold environment.[4,42]

### 3.5. Metal removal capacity of EPS

Metal tolerance capacity of Arctic strain PAMC 28620 in terms of MIC estimation results are shown in Table S2.† Of the metal ions tested, $Fe^{2+}$ ion had shown a highest MIC value about 2.0 m mol $L^{-1}$ and the remaining other metals were exhibited moderate MIC values. The metal-binding property of the EPS was critically investigated and the adsorption percentage value ($Q_e$) of each metal was determined and presented in Table 2. The results showed that $Fe^{2+}$ (99.69%), $Cu^{2+}$ (99.28%), $Mg^{2+}$ (99.19%), and $Zn^{2+}$ (98.73%) were effectively adsorbed by the EPS, whereas $Mn^{2+}$ (92.66%) and $Ca^{2+}$ (92.33) were comparatively less adsorbed onto the EPS surface. The present study has shown a high metal removal rate and it was greatly comparable with previous metal removal studies.[1,17,19,20] Therefore, the EPS from strain PAMC 28620 can be developed as an effective biosorbent for wastewater treatment.

Most of the EPSs from polar/marine bacteria are acidic polysaccharides with net negative charge, which gives an adhesive property to the EPS[1,42] and this property is significant in terms of attracting the cations such as dissolved metals from the surrounding environment.[50] Divalent metal cations are usually immobilized on the EPS matrix by co-ordinate covalent

Table 2 Metal removal by EPS produced by Arctic glacier soil bacterium *Pseudomonas* sp. PAMC 28620. The initial EPS and metal concentration (1 : 1) was 12 500 mg $L^{-1}$

| Metal ions | Final metal concentration (mg $L^{-1}$) | Metal uptake by EPS (mg $L^{-1}$) | Metal binding & removal (%) |
|---|---|---|---|
| $Mg^{2+}$ | 100.58 | 12 399.41 | 99.19 |
| $Mn^{2+}$ | 917.32 | 11 582.68 | 92.66 |
| $Fe^{2+}$ | 38.31 | 12 461.68 | 99.69 |
| $Cu^{2+}$ | 89.64 | 12 410.35 | 99.28 |
| $Zn^{2+}$ | 157.75 | 12 342.24 | 98.73 |
| $Ca^{2+}$ | 958.24 | 11 541.75 | 92.33 |

bonds which further stimulate the formation of tough EPS–metal complexes.[20,51] Our result shows that the EPS from strain PAMC 28620 can able to bind/adsorb a range of essential trace metal species (Fe, Ca, Mg, Mn, & Zn). Very few Arctic bacterial EPSs have shown to be exhibiting metal-chelating/binding capacity.[1,16] Metal-binding capacity of the EPS matrix is likely to be governed by its functional groups, such as carboxyl, hydroxyl and other ionizable competent clusters and glycosidic linkages of the polysaccharide structure.[16,18,51] Metal-binding ability is one of the essential ecological roles of the EPSs in which they would concentrate the helpful trace metal ions to the surface of the bacterium where they exist as aggregates of metallic particles.[1,2,52] In this study, $Fe^{2+}$ was more significantly adsorbed by the EPS of PAMC 28620 rather than other metals were tested. This observation also gives a solid clue about that iron (Fe) can be act as an essential factor for the primary production in Arctic bacterial populations and our results are in complete agreement with previous reports[4,22,53] and they have proposed that EPS may act as receptor or organic ligands for the iron and this process perhaps greatly affects the bioavailability of trace metals in the particular Arctic environment.

### 3.6. Metal complexation potential of EPS

FE-SEM was utilized to investigate the morphological features of the EPS before and after the adsorption experiments. The purified EPS became crystallized in the form of flake crystals and this feature was quite common in polysaccharide especially microbial EPSs. After the metal-binding experiment, the metal ions particles scattered on the EPS matrix were detected and moreover metal particles were attached with EPS flakes (data not shown). Fig. 5 shows the metal complexation after the biosorption of $Fe^{2+}$, $Cu^{2+}$, and $Ca^{2+}$ ions. The EPS and metal ion interacts together and produce metal clumps and then precipitated along with EPS. Corresponding EDX chemical maps (insets) which confirm the presence of metal ion in the EPS–metal complex. In some cases, the EPS matrix is not visible in SEM images especially for $Cu^{2+}$ (Fig. 5) and $Zn^{2+}$ (Fig. S9†) due to high rate metal complexation and further EPS matrixes were fully covered by adsorbed metal ions. The corresponding EDX chemical maps demonstrated the dispersal of metal ions on the EPS surfaces (Fig. 5 and S9†). Most of the previous studies were focused on the residual metal ion concentration after the removal process,[16,18–20,50] but did not depict the presence of metals on the EPS matrix. In contrast, our current study has provided a solid evidence for the EPS–metal complexation and further studies are required to expose the exact chemical mechanisms which involved in the metal binding and EPS–metal complexation.

### 3.7. Metal reducing potential of EPS

During the FE-SEM analysis, most of the metal ions in the EPS–metal complexes were found in reduced metallic form such as nanoparticles. FE-SEM images confirmed the clustered metallic nanoparticles (150–950 nm in diameter) on the surface of EPS matrixes. Of the metal ions tested, $Fe^{2+}$, $Cu^{2+}$, $Mg^{2+}$, and $Mn^{2+}$ were produced nanoparticles in the presence of aqueous EPS

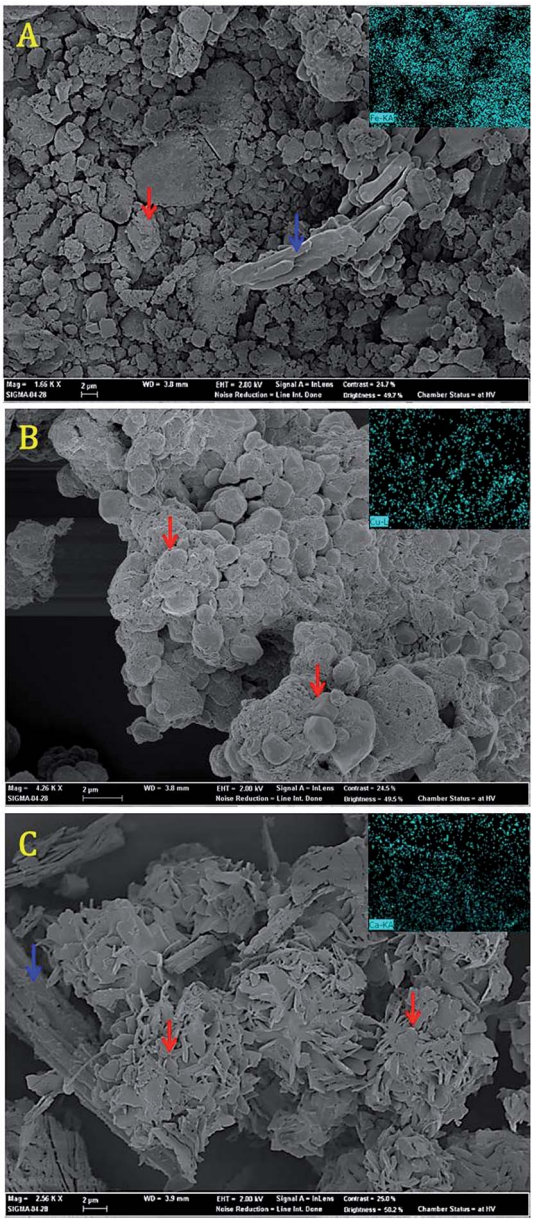


Fig. 5 FE-SEM micrograph shows the metal complexation due to EPS obtained from *Pseudomonas* sp. PAMC 28620. (A) EPS with $Fe^{2+}$, (B) EPS with $Cu^{2+}$, and (C) EPS with $Ca^{2+}$ ions. A red color arrow indicates the metal complex or aggregates produced by bacterial EPS and the blue color arrows show the EPS matrix. The EPS and metal ion interacts together and forms metal clumps and precipitated along with EPS. The insets are corresponding EDX (EDS) chemical map which confirms the metal ion distribution in the EPS–metal complex.

(50 mg $mL^{-1}$) and nanoparticles were exhibited a pattern of polycrystalline nature with different shapes (Fig. 6). The formation of metallic nanoparticles was also validated by EDX spectral analysis. Each EDX spectrum confirmed the presence of specific metal ions on the EPS matrix (Fig. 6). The result of this study suggests that EPS possibly involved as metal reducing agent for the reduction of metal ions to nanoparticles.

In recent times, hemiacetal reducing end of the monosaccharides (*i.e.*, rhamnose, galactose and glucose) of the

polysaccharide have been reported for both reduction and stabilization of inorganic nanoparticles.[24,54] Apparently, the formation of the metal nanoparticles by the action of EPS (PAMC 28620), also could be explained by a similar physiochemical mechanism. Naturally occurring nanoparticles are ubiquitous (from volcanic ash, ocean spray, fine sand & dust) and biogeochemically vital across the living planet due to their small size and large surface area dramatically affects the metal cycling.[55] Various metal reducing bacteria and their metabolites have been reported for the trace and heavy metal reduction processes for the synthesis of engineered nanoparticles.[56,57] Similarly, many bacterial EPSs including xanthan,[58] dextran,[59]

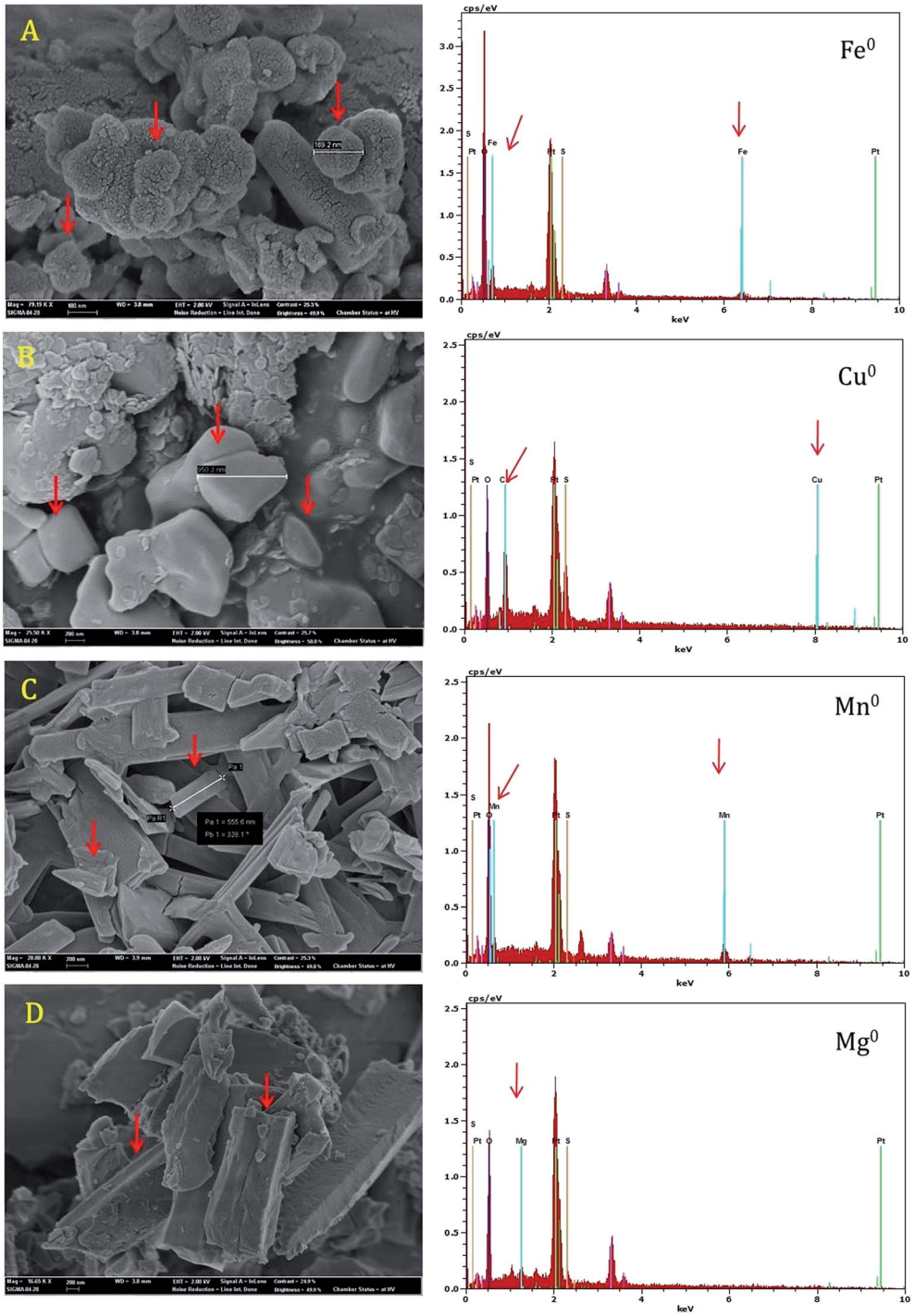


Fig. 6 FE-SEM micrograph and their corresponding EDS spectrum: metal ion reduction and the formation nanoparticle aggregates under EPS matrix. (A) $Fe^{2+}$ ions reduced into nanoparticles ($Fe^0$). (B) $Cu^{2+}$ ions reduced into nanoparticles ($Cu^0$). (C) $Mn^{2+}$ ions reduced into nanoparticles ($Mn^0$). (D) $Mg^{2+}$ ions reduced into nanoparticles ($Mg^0$). A red color arrow indicates the reduced metal ions as nanocrystals. The corresponding EDX (EDS) spectra for each metal ion were also provided (parallel) and the red color arrow indicates the presence of specific metal ion.

gellan,[60] levan,[61] succinoglycan[62] and other structurally unknown EPS[63] have been used to synthesize various metallic nanoparticles. To our knowledge, there is no report on the metal reduction led by Arctic/Antarctic bacterial EPSs. Although, the precise mechanism of reduction and stabilization of metal nanoparticles by EPS still remain to be elucidated. The behavior of trace metal nanoparticles in polar environment is needed to be explored and these nanomaterials may play a vital role in the fundamental processes at the water–mineral–cell interface in Arctic glacier environment.

## 4. Conclusions

The EPS purified from Arctic strain *Pseudomonas* sp. PAMC 28620 exhibits a distinctive and novel structural composition with rare sugars. In addition, the purified EPS had shown a significant emulsification and flocculating properties suggesting its ecological roles in the polar environments. For the first time, the metal complexation and reducing nature of EPS purified from Arctic bacterium (*Pseudomonas* sp. PAMC 28620) were analyzed. The EPS has exhibited a great capacity to bind with range of metal cations due to polyanionic nature and its metal removal potential is highly commendable. The metal ions were almost completely removed from the aqueous solution and this EPS can be used to develop an effective biosorbent for the heavy metal removal from aqueous solutions. During the metal absorption, the metal cations were reduced to nanoparticles (150–950 nm) and immobilized onto the EPS matrix. The significant effect of EPS in the metal reduction (as nanoparticles) suggests that bacterial EPS could have an important role in biogeochemical cycling of trace metals in the Arctic environment.

## Acknowledgements

The author G. Sathiyanarayanan would like to thank KU Brain Pool Fellowship Program (2016–2017) of Konkuk University, Seoul, South Korea. The study was supported by the National Research Foundation of Korea (NRF) funded by the Ministry of Education (NRF-2015R1A2A2A04006014) and (NRF-2015M1A5A1037196), and Korea Polar Research Institute (PE16030). This study is also partially supported by Advanced Production Technology Development Program, Ministry of Agriculture, Food and Rural Affairs, Republic of Korea (1201349190011).

## References

1 G. Qin, L. Zhu, X. Chen, P. G. Wang and Y. Zhang, *Microbiology*, 2007, **153**, 1566–1572.
2 M. C. A. Nichols, S. Garon, J. P. Bowman, G. Raguénès and J. Guézennec, *J. Appl. Microbiol.*, 2004, **96**, 1057–1066.
3 G. Sathiyanarayanan, D.-H. Yi, S. K. Bhatia, J.-H. Kim, H. M. Seo, Y.-G. Kim, S.-H. Park, D. Jeong, S. Jung, J.-Y. Jung, Y. K. Lee and Y. H. Yang, *RSC Adv.*, 2015, **5**, 84492–84502.
4 C. Nichols, S. Lardière, J. Bowman, P. Nichols, J. A. E. Gibson and J. Guézennec, *Microb. Ecol.*, 2005, **49**, 578–589.
5 S. Carillo, A. Casillo, G. Pieretti, E. Parrilli, F. Sannino, M. Bayer-Giraldi, S. Cosconati, E. Novellino, M. Ewert, J. W. Deming, R. Lanzetta, G. Marino, M. Parrilli, A. Randazzo, M. L. Tutino and M. M. Corsaro, *J. Am. Chem. Soc.*, 2015, **137**, 179–189.
6 M. M. Corsaro, R. Lanzetta, E. Parrilli, M. Parrilli, M. L. Tutino and S. Ummarino, *J. Bacteriol.*, 2004, **186**, 29–34.
7 A. Poli, G. Anzelmo and B. Nicolaus, *Mar. Drugs*, 2010, **8**, 1779.
8 S.-B. Liu, X.-L. Chen, H.-L. He, X.-Y. Zhang, B.-B. Xie, Y. Yu, B. Chen, B.-C. Zhou and Y.-Z. Zhang, *Appl. Environ. Microbiol.*, 2013, **79**, 224–230.
9 C. Krembs, H. Eicken, K. Junge and J. W. Deming, *Deep Sea Res., Part I*, 2002, **49**, 2163–2181.
10 A.-M. Gounot, *J. Appl. Bacteriol.*, 1991, **71**, 386–397.
11 C. Roca, V. D. Alves, F. Freitas and M. A. Reis, *Front. Microbiol.*, 2015, **6**, 288.
12 U. U. Nwodo, E. Green and A. I. Okoh, *Int. J. Mol. Sci.*, 2012, **13**, 14002–14015.
13 I. Llamas, H. Amjres, J. A. Mata, E. Quesada and V. Béjar, *Molecules*, 2012, **17**, 7103.
14 K. Okaiyeto, U. U. Nwodo, L. V. Mabinya and A. I. Okoh, *Int. J. Environ. Res. Public Health*, 2013, **10**, 5097–5110.
15 D. H. Nies, *Appl. Microbiol. Biotechnol.*, 1999, **51**, 730–750.
16 M. Loaëc, R. Olier and J. Guezennec, *Water Res.*, 1997, **31**, 1171–1179.
17 J. Morillo, M. Aguilera, A. Ramos-Cormenzana and M. Monteoliva-Sánchez, *Curr. Microbiol.*, 2006, **53**, 189–193.
18 H. Maalej, N. Hmidet, C. Boisset, L. Buon, A. Heyraud and M. Nasri, *J. Appl. Microbiol.*, 2015, **118**, 356–367.
19 J. Morillo Pérez, R. García-Ribera, T. Quesada, M. Aguilera, A. Ramos-Cormenzana and M. Monteoliva-Sánchez, *World J. Microbiol. Biotechnol.*, 2008, **24**, 2699–2704.
20 M. Polak-Berecka, D. Szwajgier and A. Waśko, *J. Food Sci.*, 2014, **79**, T2404–T2408.
21 S. Pereira, E. Micheletti, A. Zille, A. Santos, P. Moradas-Ferreira, P. Tamagnini and R. De Philippis, *Microbiology*, 2011, **157**, 451–458.
22 C. S. Hassler, E. Alasonati, C. A. Mancuso Nichols and V. I. Slaveykova, *Mar. Chem.*, 2011, **123**, 88–98.
23 O. Braissant, A. W. Decho, C. Dupraz, C. Glunk, K. M. Przekop and P. T. Visscher, *Geobiology*, 2007, **5**, 401–411.
24 F. Kang, P. J. Alvarez and D. Zhu, *Environ. Sci. Technol.*, 2014, **48**, 316–322.
25 C. E. Raja, K. Anbazhagan and G. S. Selvam, *World J. Microbiol. Biotechnol.*, 2006, **22**, 577–585.
26 S. Choudhary and P. Sar, *Bioresour. Technol.*, 2009, **100**, 2482–2492.
27 S. H. A. Hassan, R. N. N. Abskharon, S. M. F. Gad El-Rab and A. A. M. Shoreit, *J. Basic Microbiol.*, 2008, **48**, 168–176.
28 A. M. Marqués, I. Estañol, J. M. Alsina, C. Fusté, D. Simon-Pujol, J. Guinea and F. Congregado, *Appl. Environ. Microbiol.*, 1986, **52**, 1221–1223.

 

29 F. Freitas, V. D. Alves, J. Pais, M. Carvalheira, N. Costa, R. Oliveira and M. A. M. Reis, *Process Biochem.*, 2010, **45**, 297–305.

30 V. Sandhya and S. Z. Ali, *Microbiology*, 2015, **84**, 512–519.

31 G. Y. Celik, B. Aslim and Y. Beyatli, *Carbohydr. Polym.*, 2008, **73**, 178–182.

32 G. Sathiyanarayanan, V. Vignesh, G. Saibaba, A. Vinothkanna, K. Dineshkumar, M. B. Viswanathan and J. Selvin, *RSC Adv.*, 2014, **4**, 22817–22827.

33 M. DuBois, K. A. Gilles, J. K. Hamilton, P. A. Rebers and F. Smith, *Anal. Chem.*, 1956, **28**, 350–356.

34 N. R. Krieg and J. C. Holt, *Bergey's manual of systematic bacteriology*, Williams & Wilkins Co., Baltimore, 1st edn, 1984.

35 H. Jiang, H. Dong, G. Zhang, B. Yu, L. R. Chapman and M. W. Fields, *Appl. Environ. Microbiol.*, 2006, **72**, 3832–3845.

36 T. Gutierrez, T. Shimmield, C. Haidon, K. Black and D. H. Green, *Appl. Environ. Microbiol.*, 2008, **74**, 4867–4876.

37 M. M. Bradford, *Anal. Biochem.*, 1976, **72**, 248–254.

38 T. T. Terho and K. Hartiala, *Anal. Biochem.*, 1971, **41**, 471–476.

39 A. Dhasayan, J. Selvin and S. Kiran, *3 Biotech.*, 2015, **5**, 443–454.

40 W. Tang, L. Song, D. Li, J. Qiao, T. Zhao and H. Zhao, *PLoS One*, 2014, **9**, e114591.

41 G. Sathiyanarayanan, S. Filippidou, T. Junier, P. M. Rufatt, N. Jeanneret, T. Wunderlin, N. Sieber, C. Dorador and P. Junier, *AIMS Environ. Sci.*, 2016, **3**, 220–238.

42 C. A. M. Nichols, J. Guezennec and J. P. Bowman, *Mar. Biotechnol.*, 2005, **7**, 253–271.

43 M.-L. Sun, F. Zhao, M. Shi, X.-Y. Zhang, B.-C. Zhou, Y.-Z. Zhang and X.-L. Chen, *Sci. Rep.*, 2015, **5**, 18435.

44 V. Vignesh, G. Sathiyanarayanan, G. Sathishkumar, K. Parthiban, K. Sathish-Kumar and R. Thirumurugan, *RSC Adv.*, 2015, **5**, 27794–27804.

45 C. Delbarre-Ladrat, C. Sinquin, L. Lebellenger, A. Zykwinska and S. Colliec-Jouault, *Front. Chem.*, 2014, **2**, 85.

46 D.-H. Yi, G. Sathiyanarayanan, H. M. Seo, J.-H. Kim, S. K. Bhatia, Y.-G. Kim, S.-H. Park, J.-Y. Jung, Y. K. Lee and Y.-H. Yang, *Bioprocess Biosyst. Eng.*, 2016, **39**, 159–167.

47 S. Hou, J. H. Saw, K. S. Lee, T. A. Freitas, C. Belisle, Y. Kawarabayasi, S. P. Donachie, A. Pikina, M. Y. Galperin, E. V. Koonin, K. S. Makarova, M. V. Omelchenko, A. Sorokin, Y. I. Wolf, Q. X. Li, Y. S. Keum, S. Campbell, J. Denery, S.-I. Aizawa, S. Shibata, A. Malahoff and M. Alam, *Proc. Natl. Acad. Sci. U. S. A.*, 2004, **101**, 18036–18041.

48 R. P. Singh, M. K. Shukla, A. Mishra, P. Kumari, C. R. K. Reddy and B. Jha, *Carbohydr. Polym.*, 2011, **84**, 1019–1026.

49 A. Suresh Kumar, K. Mody and B. Jha, *Bull. Environ. Contam. Toxicol.*, 2007, **79**, 617–621.

50 M. J. Brown and J. N. Lester, *Water Res.*, 1982, **16**, 1539–1548.

51 X. Moppert, T. Le Costaouec, G. Raguenes, A. Courtois, C. Simon-Colin, P. Crassous, B. Costa and J. Guezennec, *J. Ind. Microbiol. Biotechnol.*, 2009, **36**, 599–604.

52 L. Norman, I. A. M. Worms, E. Angles, A. R. Bowie, C. M. Nichols, A. Ninh Pham, V. I. Slaveykova, A. T. Townsend, T. David Waite and C. S. Hassler, *Mar. Chem.*, 2015, **173**, 148–161.

53 C. S. Hassler, L. Norman, C. A. Mancuso Nichols, L. A. Clementson, C. Robinson, V. Schoemann, R. J. Watson and M. A. Doblin, *Mar. Chem.*, 2015, **173**, 136–147.

54 P. Raveendran, J. Fu and S. L. Wallen, *J. Am. Chem. Soc.*, 2003, **125**, 13940–13941.

55 E. S. Bernhardt, B. P. Colman, M. F. Hochella, B. J. Cardinale, R. M. Nisbet, C. J. Richardson and L. Yin, *J. Environ. Qual.*, 2010, **39**, 1–12.

56 N. I. Hulkoti and T. C. Taranath, *Colloids Surf., B*, 2014, **121**, 474–483.

57 S. Iravani, *Int. Scholarly Res. Not.*, 2014, **2014**, 18.

58 D. Pooja, S. Panyaram, H. Kulhari, S. S. Rachamalla and R. Sistla, *Carbohydr. Polym.*, 2014, **110**, 1–9.

59 M. Khalkhali, S. Sadighian, K. Rostamizadeh, F. Khoeini, M. Naghibi, N. Bayat, M. Habibizadeh and M. Hamidi, *BioImpacts*, 2015, **5**, 141–150.

60 S. Dhar, V. Mali, S. Bodhankar, A. Shiras, B. L. V. Prasad and V. Pokharkar, *J. Appl. Toxicol.*, 2011, **31**, 411–420.

61 K. B. A. Ahmed, D. Kalla, K. B. Uppuluri and V. Anbazhagan, *Carbohydr. Polym.*, 2014, **112**, 539–545.

62 C. Kwon, B. Park, H. Kim and S. Jung, *Bull. Korean Chem. Soc.*, 2009, **30**, 1651.

63 V. Vignesh, G. Sathiyanarayanan, G. Sathishkumar, K. Parthiban, K. Sathish-Kumar and R. Thirumurugan, *RSC Adv.*, 2015, **5**, 27794–27804.